Development 139, 4613-4622 (2012) doi:10.1242/dev.086769

Residual body removal during spermatogenesis in *C. elegans* requires genes that mediate cell corpse clearance

Jie Huang[1,2,*], Haibin Wang[3,4,*], Yingyu Chen[2], Xiaochen Wang[4,‡] and Hong Zhang[1,4,‡]

SUMMARY

Generation of spermatozoa involves segregation of most of the cytoplasm into residual bodies, which are detached from spermatids and eliminated in mammals. However, the molecular and cellular mechanism underlying the removal of residual bodies remains largely unknown. Here, we demonstrate that during *C. elegans* spermatogenesis residual bodies are engulfed and degraded by gonadal sheath cells, a process that uses the same set of genes underlying apoptotic cell removal. The two partially redundant engulfment pathways that clear cell corpses also mediate phagocytosis of residual bodies, possibly by recognizing the 'eat me' signal phosphatidylserine exposed on the surface. The residual body-containing phagosome undergoes a maturation process involving sequential steps including dynamic coating with PtdIns(3)P and association of RAB small GTPases. The genetic hierarchy of residual body removal in hermaphrodites is similar to that of cell corpse clearance, but male residual body removal involves a distinct hierarchy, with differential use of the engulfment genes. Efficient removal of residual bodies regulates the number of spermatids and effective transfer of spermatids during male matings. Our results indicate that a similar molecular mechanism is employed for the removal of residual bodies and apoptotic cell corpses in *C. elegans*.

KEY WORDS: Residual body, PS, Engulfment, Phagosome, Autophagy, *C. elegans*

INTRODUCTION

In mammals, spermatogenesis is a multistep processes, comprising mitotic proliferation of spermatogonia, meiotic division of spermatocytes and maturation of haploid spermatids (Nakanishi and Shiratsuchi, 2004). As spermatids undergo terminal differentiation into spermatozoa, the bulk cytoplasmic contents are segregated into the residual body, which is sloughed off, phagocytosed and degraded by Sertoli cells (Breucker et al., 1985; Blanco-Rodríguez and Martinez-Garcia, 1999). In *C. elegans*, spermatogenesis occurs in both males and hermaphrodites (Schedl, 1997). Upon entering meiosis, primary spermatocytes (spermatogonia) bud off the syncytial cytoplasmic core, known as the rachis, and undergo the first meiotic division, resulting in the generation of two secondary spermatocytes that may or may not remain attached by a cytoplasmic bridge (Ward, 1986). Nevertheless, the resulting secondary spermatocytes initiate meiosis II to produce two haploid spermatids and one residual body (Fig. 1A). The cytosolic components are differentially partitioned into developing spermatids and the residual body. Spermatids inherit mitochondria, Golgi-derived fibrous-body membranous organelles (FB-MOs) and a haploid nucleus, whereas all ribosomes, nearly all actin and myosin and most of the tubulin, are packaged into the residual body (Ward, 1986; Ward et al., 1983; Machaca et al., 1996). *C. elegans* spermatogenesis occurs in the absence of cells functioning as Sertoli cells, which separate different stages of spermatogenesis into distinct compartments in mammals (Nakanishi and Shiratsuchi, 2004). Little is known about the molecular and cellular mechanisms underlying the clearance of residual bodies.

During *C. elegans* development, 131 somatic cells undergo apoptosis and the apoptotic cell corpses are removed by neighboring cells (Sulston and Horvitz, 1977; Sulston et al., 1983). Following recognition of the 'eat me' signal phosphatidylserine (PS) on the surface of cell corpses, phagocytic cells extend pseudopods, then envelop and internalize the cell corpse to form a phagosome (Zhou and Yu, 2008; Kinchen and Ravichandran, 2008). Recognition and phagocytosis of cell corpses are mediated by two partially redundant signaling pathways with *psr-1*, *ina-1*, *ced-2*, *ced-5*, *ced-12* and *ced-10* in one pathway and *ttr-52*, *ced-1*, *ced-7*, *ced-6* and *dyn-1* in the other (Fig. 1B) (Zhou and Yu, 2008; Kinchen and Ravichandran, 2008; Yu et al., 2006; Wang et al., 2010; Hsu and Wu, 2010; Wang et al., 2003). CED-2 (CrkII in mammals), CED-5 (Dock180; also known as Dock1) and CED-12 (ELMO) mediate the engulfment signal received by upstream receptors such as PSR-1 and INA-1 to activate CED-10 (Rac1), which regulates the cytoskeleton rearrangement of engulfing cells (Reddien and Horvitz, 2000; Wu and Horvitz, 1998b; Wu et al., 2001; Zhou et al., 2001a; Gumienny et al., 2001). The secreted bridging molecule TTR-52, transmembrane scavenger-receptor-like protein CED-1 (mammalian LRP1/MEGF10), an ATP-binding cassette transporter CED-7 (ABCA1 and ABCA7) and the secreted LPS-binding/lipid transfer family protein NRF-5 regulate the initial recognition of apoptotic cells. The signal is transduced by the adaptor protein CED-6 (GULP), which may also converge on CED-10 to coordinately regulate the actin cytoskeleton (Wang et al., 2010; Zhou et al., 2001b; Liu and Hengartner, 1998; Wu and Horvitz, 1998a; Kinchen et al., 2005; Zhang et al., 2012). Maturation of nascent cell corpse-containing phagosomes involves dynamic association of PdtIns(3)P and sequential recruitment of Rab small GTPases, including RAB-5, RAB-7, UNC-108/RAB2 and RAB-14, that mediate the stepwise maturation processes,

[1]State Key Laboratory of Biomacromolecules, Institute of Biophysics, Chinese Academy of Sciences, Beijing, 100101, P.R. China. [2]Key Laboratory of Medical Immunology, Ministry of Health, Peking University Health Science Center, Beijing, 100191, P.R. China. [3]College of Life Sciences, China Agricultural University, Beijing, 100094, P.R. China. [4]National Institute of Biological Sciences, Beijing, 102206, P.R. China.

*These authors contributed equally to this work
‡Authors for correspondence (wangxiaochen@nibs.ac.cn; hongzhang@sun5.ibp.ac.cn)

Accepted 21 September 2012

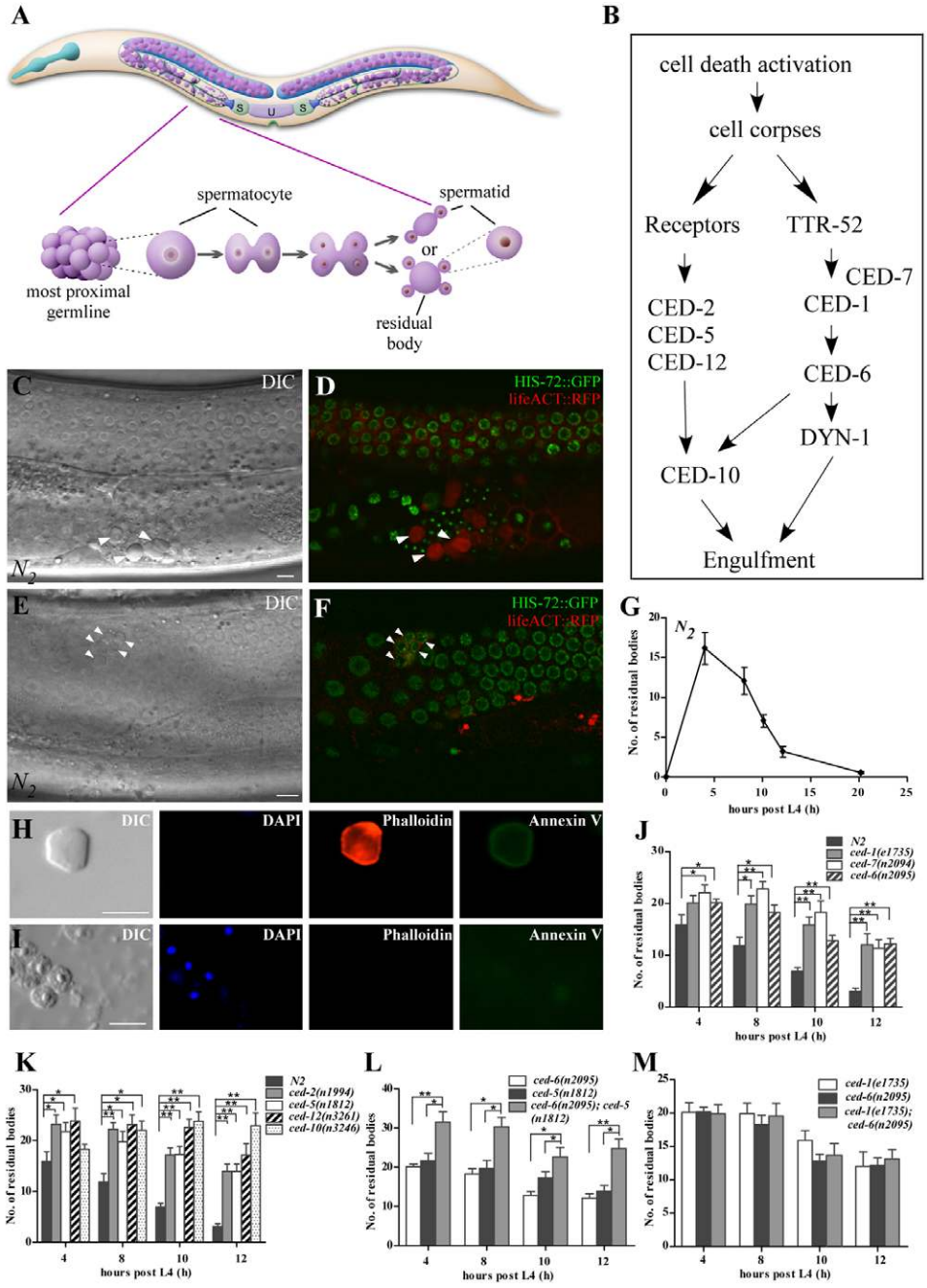

Fig. 1. Engulfment mutants accumulate residual bodies. (**A**) Schematic of the hermaphrodite germline and spermatogenesis process. Primary spermatocytes, residual bodies associated with non-budding spermatids and single spermatids, are shown in the proximal gonad. Light green (S), spermatheca; light purple (U), uterus; blue lines, pairs of gonadal sheath cells. The meiosis process is shown underneath. Primary spermatocytes (spermatogonia) bud off the syncytial cytoplasmic core, known as the rachis, and undergo meiosis, resulting in generation of 2N secondary spermatocytes that sometimes undergo incomplete cytokinesis and remain attached. During meiosis II, each of the resulting secondary spermatocytes produces two haploid spermatids and one residual body. Spermatids form by budding form an anucleate residual body. (**B**) Schematic of the two partially redundant cell corpse engulfment pathways. (**C**,**D**) DIC (C) and fluorescent (D) images of a wild-type worm carrying $P_{his\text{-}72}$HIS-72::GFP and $P_{pie\text{-}1}$lifeACT::RFP. Residual bodies in the right arm of the gonad (arrowheads) are identified by their button-like morphology under Nomarski optics (C) and labeling by lifeACT::RFP (actin) but not HIS-72::GFP (chromatin) (D). In this study, the head of the animal was shown anterior and the tail was located posterior. (**E**,**F**) Germ cell corpses in the loop region of the left arm of the gonad (arrowheads) are identified by their button-like morphology under Nomarski optics (E) and labeling by HIS-72::GFP in nuclei and lifeACT::RFP on the cell membrane (F). (**G**) Quantification of residual bodies. Five different time points post L4 stage (4, 8, 10, 12 and 20 hours) were examined in one gonad arm in wild type (N2). At least 15 worms were scored at each time point. Error bars represent s.e.m. (**H**,**I**) Residual bodies (H) but not spermatids (I) are stained by Annexin V. Residual bodies are stained by phalloidin (which labels actin filaments) but not DAPI (which labels nuclear DNA), whereas spermatids are positive for DAPI but not phalloidin. About 77.4% residual bodies (n=53) were stained by Annexin V. (**J-M**) Residual bodies were scored at different time points from one gonad arm in the indicated strains. At least 15 animals were scored in each strain at each time point. Data are shown as mean±s.e.m. Data derived from *ced* mutants are compared with wild type (N2) in J and K by unpaired t-test, whereas single *ced* mutants are compared with double mutants in L and M. *P<0.05, **P<0.0001. Scale bars: 5 μm.

resulting in extensive remodeling of phagosomal membranes and contents before fusion with lysosomes for degradation (Zhou and Yu, 2008; Kinchen and Ravichandran, 2008; Guo et al., 2010).

Here, we demonstrated that in *C. elegans*, cell corpse removal and the clearance of residual bodies during spermatogenesis are mediated by a common set of genes. Residual bodies expose PS on the surface and are phagocytosed by the gonadal epithelial sheath cells, a process regulated by cell corpse engulfment genes. The residual body-containing phagosomes undergo a series of maturation processes involving sequential association of small GTPases to form degradative phagolysosomes. Interestingly, whereas residual body removal in hermaphrodites shares a genetic hierarchy with cell corpse clearance, male residual body removal involves differential use of the engulfment genes, which form a distinct hierarchy. Mutant hermaphrodites and males with accumulated residual bodies contain fewer spermatids. Mutant males also exhibit a defect in transfer of spermatids during mating, thus reducing the mating efficiency. Our results provide insights into the removal of residual bodies in other organisms.

MATERIALS AND METHODS

C. elegans strains

Strains of *C. elegans* were cultured at 20°C using standard protocols. The wild-type strain was N2 Bristol. Mutant alleles used in this study are listed below. LGI: *ced-1(e1735)*, *ced-12(n3261)*, *unc-108(n3263)*. LGII: *laat-1(qx42)*, *lgg-1(bp500)*. LGIII: *ced-6(n2095)*, *ced-7(n2094)*, *ttr-52(tm2078)*, *epg-3(bp405)*. LGIV: *ced-2(n1994)*, *ced-5(n1812)*, *ced-10(n3246)*. LGV: *fog-2(q71)*, *him-5(e1490)*. LGX: *piki-1(ok2346)*, *ceh-18(mg57)*, *rab-14(tm2095)*, *atg-2(bp576)*. Strains carrying integrated arrays used in this study include *smIs34*(P_{ced-1}CED-1::GFP), *opIs334*(P_{ced-1}YFP::2xFYVE), *bcIs39*(P_{lim-7}CED-1::GFP), *qxIs66*(P_{ced-1}GFP::RAB-7), *qxIs408*(P_{ced-1}GFP::RAB-5), *qxIs405*(P_{ced-1}GFP::ACT-1), *qxIs354*(P_{ced-1}LAAT-1::GFP), *zbIs2*(P_{pie-1}lifeACT::RFP), *yqIs100*(P_{ced-1}mCHERRY::ACT-1), *qxIs68* (P_{ced-1}mCHERRY::RAB-7), *qxIs352*(P_{ced-1}LAAT-1::nCHERRY) and *stIs10027*(P_{his-72}HIS-72::GFP).

Quantification of residual bodies

In hermaphrodites, residual bodies were counted in the proximal gonad arm at four different time points using Nomarski optics. The number of residual bodies in males was quantified in strains carrying the *him-5(e1492)* mutation, which increases the frequency of X chromosome non-disjunction and thus increases the frequency of XO males in self-fertile populations.

Quantification of cell corpses

The numbers of cell corpses in the head region of living embryos were scored using Nomarski optics as described previously (Parrish et al., 2001).

RNA interference (RNAi) experiments

RNAi experiments were carried out by bacterial feeding as described previously (Kamath and Ahringer, 2003). L4 animals were treated with RNAi for *vps-34* (pPD129.36-*vps-34*), *rab-5* or *rab-7*, and L4 larvae of the F1 generation were transferred to fresh RNAi plates and aged for 4, 8, 10 or 12 hours before examination.

Annexin V and phalloidin staining

Annexin V staining was performed as described previously with modifications (Wang et al., 2007). Hermaphrodites or males were dissected in a 40 μl drop of sperm medium (SM) buffer (50 mM HEPES, 25 mM KCl, 45 mM NaCl, 1 mM $MgSO_4$, 5 mM $CaCl_2$, 10 mM dextrose; pH 7.8) containing 0.5 μl Alexa Fluor 488-conjugated Annexin V (Molecular Probes, Eugene, OR, USA) on a slide freshly coated with poly-lysine to release residual bodies and sperm, and incubated for 20 minutes at room temperature. The dye was washed with SM buffer three times. The samples were then incubated in 30 μl of 4% paraformaldehyde for 15 minutes and in 4% paraformaldehyde containing 5% Triton X-100 for 10 minutes. A coverslip was placed on top of the sample, and the slide was frozen on a block that had been cooled in liquid nitrogen while applying gentle pressure to remove the coverslip. The samples were rinsed three times for 15 minutes each in PBST (1.4 M NaCl, 0.03 M KCl, 0.1 M Na_2HPO_4, 0.02 M KH_2PO_4, 0.2% Tween 20, pH 7.2) containing 10 mg/ml glycine to block unreacted aldehydes. After incubating for 1 hour in PBS containing 1% BSA and 10% serum, the sample was incubated with rhodamine-conjugated phalloidin (Molecular Probes, Life Technologies) for 2 hours, and then washed with PBS for 15 minutes. Finally, the sample was incubated in DAPI, coverslipped and sealed with nail polish. Slides were viewed using an epifluorescence microscope or a confocal microscope (Zeiss LSM 510 Meta plus Zeiss Axiovert zoom).

Ovulation rate analysis

Animals were mounted in M9 buffer (22 mM KH_2PO_4, 42 mM Na_2HPO_4, 86 mM NaCl, 1 mM $MgSO_4$) and the total number of embryos in the uterus of each animals was counted using Nomarski optics. Animals were then transferred to fresh plates with *Escherichia coli* for the indicated interval. Embryos in the uterus and laid on the plate were determined. Twenty animals were scored for each genotype. The time interval for adult worms (10 hours post L4) was 3.5 hours and for young adult worms (2 hours post L4) was 5.5 hours. The ovulation rate per gonad arm per hour = (number of embryos at the end of interval – number of embryos at the beginning of interval)/(2×number of animals scored for this genotype×time interval).

Spermatid quantification assay

For both wild-type and mutant animals, the *his-72::GFP* transgene was included to facilitate the counting. A single hermaphrodite (4 hours post L4) or a single male (10 hours post L4) was picked into a small drop of SM buffer on a slide. The coverslip was placed gently on the drop and the animal was crushed to release sperm. The number of HIS-72::GFP-marked sperm was counted using a epifluorescence microscope. At least ten worms were scored for each genotype.

Mating assay

Ten wild-type or ten mutant males at the L4 stage were picked and placed on fresh plates for 24 hours before mating with three *unc-76* hermaphrodites overnight. Each hermaphrodite was transferred to a new plate and the progeny were quantified.

dpy-5 hermaphrodites at the L4 larval stage were individually picked to fresh plates and were allowed to produce self-progeny for 1 day. The hermaphrodite was then transferred to a fresh plate with a small spot of *E. coli* (mating plate) and was mated overnight with four wild-type or mutant males at 36 hours post L4 stage. Each hermaphrodite was transferred to a new plate for the next 4 days. The progeny produced each day were determined. At least 14 crosses were performed for each strain.

To measure the number of spermatids in matings, one mutant or wild-type male at 24 hours post L4 was picked and mated with ten virgin *fog-2; ceh-18* females. The animals were transferred individually to separate plates as soon as fertilized eggs were observed on the mating plate. The total progeny were counted to determine the number of sperm transferred per mating for a given mated female.

In vitro sperm activation assay

L4 stage males with rounded tails were picked and placed on fresh plates and grew for a day or two. The celibate males were transferred to a new plate without bacteria and allowed to crawl for few minutes. A slide was marked with a small circle using a PAP pen, and then 30-50 μl of SM buffer containing Pronase E (20 μg/ml) was added within the circle in which about ten males were transferred. Animals were cut by needles to release spermatids. After 5 minutes for activation, a coverslip was gently placed on the surface of dissected sample and spermatids or spermatozoa were observed using a 100× oil immersion lens.

Confocal microscopy

Time-lapse recording was performed using a Zeiss LSM 510 Pascal inverted confocal microscope with 488/543 lasers (Carl Zeiss) and images were processed and viewed using LSM Image Browser software. Animals at 6-8 hours post L4 were mounted on agar pads and images in a 15–17 *z* series (1.1 mm/section) were captured every 1.5 minutes or 2 minutes for 120 minutes (Carl Zeiss).

Statistical analysis

The standard error of the mean (s.e.m.) was used as the *y* error bar for bar charts plotted from the mean value of the data. Data derived from different genetic backgrounds were compared using Student's two way unpaired *t*-test. Data were considered statistically different at $P<0.05$.

RESULTS

Monitoring residual bodies in vivo

C. elegans hermaphrodites contain two symmetric U-shaped gonad arms connected by the uterus. Spermatogenesis initiates at the L4 larval stage and generates 180-300 haploid spermatids, which accumulate in the proximal gonad arm (Fig. 1A). Hermaphrodites cease spermatogenesis and switch to oogenesis at the adult stage. The first ovulation pushes spermatids out of the gonad and into the spermatheca, where they differentiate into spermatozoa (Fig. 1A) (Schedl, 1997; L'Hernault, 2006). We followed spermatogenesis by time-lapse recording and found that the residual body appears as a 'button-like' body in the proximal gonad under DIC (Nomarski differential interference contrast microscopy) (Fig. 1C; supplementary material Fig. S1A). Residual bodies are distinct from germ cell corpses, which are restricted to the bend region of the U-shaped gonad arm (Fig. 1E) (Gumienny et al., 1999). Residual bodies lack chromatin structures but inherit almost all the actin and tubulin from the spermatocyte (Ward, 1986). We used the HIS-72::GFP and lifeACT::RFP reporters, which label chromatin and actin, respectively, to identify residual bodies. The 'button-like' residual bodies visible by DIC in the proximal gonad are labeled by lifeACT::RFP but not HIS-72::GFP (Fig. 1C,D), whereas the germ cell corpses with the similar 'button-like' structures in the loop region of the gonad arm are stained by HIS-72::GFP in nuclear and lifeACT::RFP near the cell surface (Fig. 1E,F). Expulsion of the newly fertilized oocyte out of the spermatheca displaces many spermatozoa into the uterus that rapidly crawl back into the spermatheca (Ward and Carrel, 1979). We also observed that some residual bodies were pushed into the uterus by the passing oocytes, but these 'non-motile' residual bodies did not crawl back into the spermatheca (supplementary material Fig. S1C).

We quantified the number of residual bodies in the proximal gonad arm at different developmental times (Fig. 1G). Residual bodies reached a maximum number at 4 hours post L4 stage, consistent with the generation of spermatids at this time point, and were hardly observed 20 hours post L4 (Fig. 1G; supplementary material Fig. S1D). Time-lapse recording revealed that residual bodies disappeared in about 64 minutes (supplementary material Fig. S1A), indicating that they are removed or lysed during development.

Mutants with defective removal of apoptotic cell corpses accumulate residual bodies

We examined whether mutants with defects in apoptotic cell removal impair the clearance of residual bodies. We found significantly more residual bodies in the gonad arm immediately distal to the spermatheca in engulfment mutants than in wild type at every time point examined (Fig. 1J,K; supplementary material Fig. S1E). Consistent with this observation, residual bodies were found to persist much longer in *ced-1* mutants than in wild type (supplementary material Fig. S1B). Double mutants of genes acting in the two different pathways, including *ced-6(n2095); ced-5(n1812)*, *ced-1(e1735); ced-2(n1994)* and *ced-1(e1735); ced-5(n1812)*, accumulated more residual bodies than single mutants, whereas double mutants of genes acting in the same pathway exhibited no increase (Fig. 1L,M; supplementary material Fig. S1F-H). The secreted PS-binding proteins TTR-52 and NRF-5, which are required for mediating apoptotic cell recognition, did not show obvious residual body removal defect (supplementary material Fig. S1I). Thus, the two engulfment pathways act in parallel in the removal of residual bodies. Engulfment defective *ced* mutants exhibited a similar ovulation rate to wild-type animals, ruling out the possibility that residual bodies are simply expelled by the passing oocytes and further suggests that residual bodies are engulfed and degraded by other cells (supplementary material Fig. S1J,K).

Phosphatidylserine (PS) is exposed on the surface of apoptotic cells and serves as an 'eat me' signal for clearance (Wang et al., 2007; Wang et al., 2010). We determined next whether residual bodies expose PS on the surface by staining with fluorescent-conjugated Annexin V, a highly specific phosphatidylserine-binding protein (Wang et al., 2007). The residual body, labeled by phalloidin (which stains actin) but not DAPI (which stains nuclei), had bright ring-shaped Annexin V staining, whereas the spermatid remained unlabeled by Annexin V (Fig. 1H,I), indicating that PS is exposed on the surface of residual bodies but not of spermatids.

Loss of function in genes essential for programmed cell death, including *ced-3*, *ced-4* and *egl-1*, did not affect the removal of or suppress the accumulation of residual bodies in *ced-1* mutants (supplementary material Fig. S2A-C). Mutations in genes required for the autophagy pathway, which is a lysosome-mediated degradation system (Tian et al., 2010), also caused no evident defect in the clearance of residual bodies (supplementary material Fig. S2D).

Residual bodies are engulfed by gonadal sheath cells

During cell corpse removal, the engulfment genes regulate the extension of pseudopods from engulfing cells along the surface of cell corpses, which are eventually internalized and enclosed within phagosomes in the phagocytes, accompanied by reorganization of the actin cytoskeleton (Zhou and Yu, 2008; Kinchen and Ravichandran, 2008). CED-1 localizes to the extending pseudopods and nascent phagosomes (Zhou et al., 2001b). We found that CED-1::GFP clustered around residual bodies, which are positive for lifeACT::RFP (actin) but not HIS-72::GFP (chromatin), and was absent from HIS-72::GFP-labeled spermatids (Fig. 2A-D). GFP::ACT-1, which is expressed in phagocytes and indicates the initial cytoskeleton change, also surrounded residual bodies (Fig. 2E,F).

In hermaphrodites, five pairs of single-layer gonadal sheath cells cover each gonadal arm, serving as the sole phagocytic cells for clearing germ cell corpses (Fig. 1A) (Gumienny et al., 1999). To determine whether residual bodies are also phagocytosed by sheath cells, we examined the expression of CED-1::GFP, which is driven by the sheath cell-specific promoter *lim-7* ($P_{lim\text{-}7}$CED-1::GFP), and found that residual bodies were surrounded by CED-1::GFP (Fig. 2G,H). The residual bodies displaced from the uterus by fertilization were also labeled by sheath cell-expressed CED-1::GFP (supplementary material Fig. S1L,M), indicating that sheath cells can extend pseudopods into the uterus. The defective removal of residual bodies in *ced-1* mutants was fully rescued by the $P_{lim\text{-}7}$*ced-1::gfp* transgene (Fig. 2I), confirming that gonadal sheath cells are the main phagocytic cells for removing residual bodies.

PtdIns(3)P and Rab GTPases are required for maturation of residual body-containing phagosomes

We next examined the maturation of residual body-containing phagosomes. In the proximal gonad, 36.2% of residual bodies were

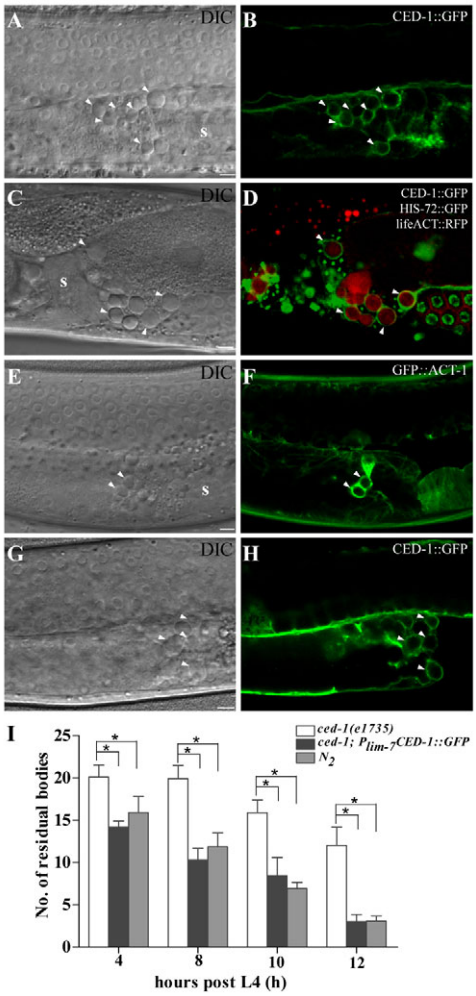

Fig. 2. Residual bodies are engulfed by gonadal sheath cells. (**A-D**) DIC (A,C) and fluorescence (B,D) images of wild-type worms carrying CED-1::GFP (A,B) or CED-1::GFP, HIS-72::GFP and lifeACT::RFP (C,D). CED-1::GFP clusters around button-like residual bodies positive for lifeACT::RFP but not HIS-72::GFP (arrowheads). The left gonadal arm is shown in A and B, and a right gonadal arm is shown in C and D. (**E-H**) DIC (E,G) and fluorescence (F,H) images of wild-type animals carrying P_{ced-1}GFP::ACT-1 (E,F) or P_{lim-7}CED-1::GFP (G,H). Residual bodies (arrowheads) are labeled by GFP::ACT-1 expressed in engulfing cells (E,F) and CED-1::GFP expressed specifically in gonadal sheath cells (G,H). The left gonadal arm is shown. (**I**) Expression of CED-1::GFP in sheath cells fully rescues the accumulation of residual bodies in *ced-1(e1735)* mutants. The numbers of residual bodies were scored at four different time points post L4 (15 animals each). Data are shown as mean±s.e.m. *P<0.05. s, spermatheca. Scale bars: 5 μm.

labeled by the PtdIns(3)P-binding protein YFP::2xFYVE (Fig. 3A-C), indicating accumulation of PtdIns(3)P on the surface of residual body-containing phagosomes. Loss of VPS-34 and PIKI-1, the two PtdIns(3)P kinases (Zou et al., 2009), reduced the labeling of YFP::2xFYVE to 17.9% and 0.6%, respectively, and caused accumulation of residual bodies (Fig. 3C,F,I), consistent with the essential role of PtdIns(3)P in phagosome maturation. The milder defect in *vps-34(RNAi)* animals compared with *piki-1(ok2346)* might be due to inefficient knockdown of *vps-34* activity by RNAi feeding or might indicate a more important role of *piki-1* in the maturation of residual body-containing phagosomes in gonadal sheath cells.

The association of small GTPases with residual body-containing phagosomes was also examined. GFP::RAB-5, which is expressed in the phagocytes including gonadal sheath cells, was enriched on residual bodies-containing phagosomes (Fig. 3D,E). Inactivation of *rab-5* reduced YFP::2xFYVE labeling on phagosomes and caused accumulation of residual bodies (Fig. 3C,I). GFP::RAB-7 and the lysosomal membrane protein LAAT-1 also formed rings around residual bodies (Fig. 3G,H,J,K) and loss of their functions resulted in accumulation of residual bodies (Fig. 3F,I) (Liu et al., 2012). Mutations in *rab-14* and *unc-108/RAB2* also caused defective residual body clearance, which was further enhanced in *unc-108(n3263); rab-14(tm2095)* double mutants (Fig. 3F,L), consistent with the redundant roles of UNC-108 and RAB-14 in regulating phagosome maturation (Guo et al., 2010; Lu et al., 2008; Mangahas et al., 2008).

The temporal order of recruitment of these factors to residual body-containing phagosomes was determined by time-lapse recording. In wild type, CED-1::GFP, the phagocytic receptor, clustered around residual bodies and formed a full ring within 2-7 minutes (Fig. 4A). ACT-1, which indicates the first cytoskeleton change in the phagocytic cells and phagocytic cup formation, showed identical behavior with CED-1::GFP (data not shown). The ACT-1 reporters were used to monitor sequential events with other phagosome markers. YFP::2xFYVE became enriched on the residual body 7 minutes after the closure of the phagosome labeled by mCHERRY::ACT-1 and persisted for an average of 60 minutes (Fig. 4B,F). Multiple waves of FYVE recruitment were observed in ~50% of residual body-containing phagosomes. RAB-5 and RAB-7 appeared on the surface 9 and 13 minutes, respectively, after phagosome formation (Fig. 4C,D,F). LAAT-1 was the last to be recruited at 36 minutes after phagosome formation and it persisted until the residual bodies were degraded (Fig. 4E,F). Thus, PtdIns(3)P and small GTPases are sequentially recruited to the residual body-containing phagosomes in an order similar to that during degradation of apoptotic cell corpses (Fig. 4F).

Engulfment genes are differentially required for removal of residual bodies in males

The male gonad is a single-lobed structure (Fig. 5A). Spermatogenesis occurs in the proximal germline from the L4 larval stage onwards and spermatids are stored in the seminal vesicle until ejaculation (Schedl, 1997). Residual bodies, which appeared as 'button-like' structures labeled by lifeACT::RFP (actin) but not HIS-72::GFP (chromatin), accumulated in the proximal gonad region and reached a maximum number at 36 hours post L4 stage (Fig. 5B-D; supplementary material Fig. S3A). The number of residual bodies remained high during later stages, consistent with constitutive spermatid generation in males.

We investigated whether engulfment genes also regulate the removal of residual bodies in males. Residual bodies, which exposed PS on the surface as revealed by Annexin V staining, accumulated in engulfment-defective mutants (Fig. 5E-G; supplementary material Fig. S3B,C). Interestingly, *ced-6* mutants exhibited a much milder defect than *ced-1* mutants, whereas *ced-7* and *ttr-52* males appeared to be normal (Fig. 5F). *ced-2*, *ced-5* and *ced-10* mutants also showed a milder clearance defect than *ced-1* mutants (Fig. 5F,G). Moreover, *ced-5(n1812)*, *ced-2(n1994)* or *ced-6(n2095)* did not further enhance the engulfment defect in *ced-1(e1735)* mutants, whereas the number of residual bodies in *ced-6(n2095); ced-5(n1812)* double mutants was significantly higher than either of the single mutants alone but was similar to that in

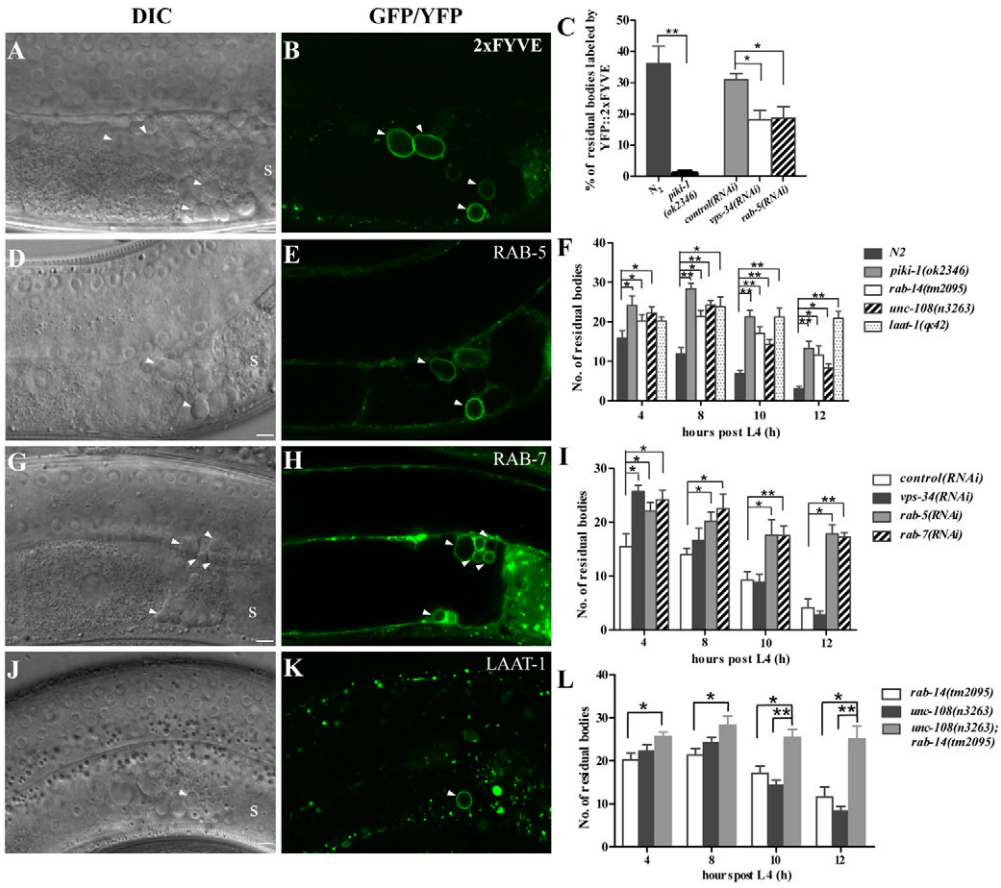

Fig. 3. PtdIns(3)P and Rab GTPases are required for the maturation of residual body-containing phagosomes. (**A**,**B**,**D**,**E**,**G**,**H**,**J**,**K**) DIC and fluorescence images of wild-type worms carrying $P_{ced\text{-}1}$YFP::2xFYVE (A,B), $P_{ced\text{-}1}$GFP::RAB-5 (D,E), $P_{ced\text{-}1}$GFP::RAB-7 (G,H) or $P_{ced\text{-}1}$LAAT-1::GFP (J,K). Residual bodies (arrowheads) are labeled by YFP::2xFYVE, GFP::RAB-5, GFP::RAB-7 and LAAT-1::GFP, respectively. In A, B, G, H, J and K, the left gonadal arm is shown; in D and E, the right gonadal arm is shown. (**C**) The percentage of residual bodies labeled by YFP::2xFYVE was quantified in the indicated strains at 7 hours post L4 stage. At least 15 animals were scored in each strain. (**F**,**I**,**L**) Residual bodies were scored in the indicated strains at four different time points (4, 8, 10 and 12 hours) post L4 stage. At least 15 animals were scored in each strain at each time point. In panels C, F, I and L, data derived from mutant backgrounds or RNAi treated animals were compared with wild type or control RNAi. $^{**}P<0.0001$, $^{*}P<0.05$. Data are shown as mean±s.e.m. Scale bars: 5 μm.

ced-1 mutants (Fig. 5H,I; supplementary material Fig. S3D-F). These data suggest that *ced-1* is the most upstream gene, whereas *ced-2*, *ced-5* and *ced-6* act in parallel, but downstream of *ced-1*, to remove residual bodies in males. Loss of *ttr-52* or *ced-7* did not cause obvious defects in residual body clearance or enhance the defect of *ced-2* or *ced-5* mutants, suggesting that they are likely to be dispensable for this process in males (Fig. 5F; supplementary material Fig. S3G,H). By contrast, loss of *ced-12* significantly enhanced the residual body clearance defect of *ced-6* mutants, albeit displaying no obvious phenotype on its own (Fig. 5G; supplementary material Fig. S3I), indicating that *ced-12* might play a minor role in residual body removal in males. Consistent with this, no abnormal accumulation of residual bodies was observed in *ced-12; ttr-52* or *ced-12; ced-7* double mutants (supplementary material Fig. S3J,K). The defective clearance of residual bodies in *ced-1* mutants was rescued by $P_{lim\text{-}7}$CED-1::GFP-expressed *ced-1* (Fig. 5J), indicating that residual bodies in males are also engulfed by sheath cell-like cells. Taken together, these data indicate that engulfment genes are differentially required to remove residual bodies in males and hermaphrodites.

As in hermaphrodites, residual bodies accumulated in males defective in phagosome maturation, including those lacking *rab-5*, *rab-7*, *vps-34*, *piki-1* or *unc-108* (Fig. 5K,L; supplementary material Fig. S3L). *laat-1* and *rab-14* mutants exhibited a milder defect (supplementary material Fig. S3M), suggesting that redundant components are involved in this process. CED-1::GFP, YFP::2xFYVE, GFP::RAB-5, GFP::RAB-7 and LAAT-1::GFP also coated the surface of residual body-containing phagosomes in males, with a similar sequential order as in hermaphrodites (supplementary material Fig. S4). However, the phagosomal degradation of residual bodies was much more efficient in males, taking only 30 minutes, compared with about 70 minutes in hermaphrodites.

Removal of residual bodies regulates the number of spermatids and male mating efficiency

We examined the number of sperm in mutant hermaphrodites and males with accumulated residual bodies. *ced-1(e1735)*, *ced-5(n1812)*, *ced-6(n2095)*, *unc-108(n3263)* and *rab-14(tm2095)* mutant hermaphrodites contained significantly reduced numbers of spermatids compared with wild type at 4 hours post L4 (Fig. 6A). The *ced-1* mutant males also contained far fewer spermatids at 10 hours post L4 (Fig. 6B). The number of spermatids in *ced-1* mutant hermaphrodites was rescued by $P_{lim\text{-}7}$*ced-1::gfp* (Fig. 6A). These results indicate that defective clearance of residual bodies reduces the number of spermatids.

We performed a sperm competition assay to investigate whether accumulation of residual bodies has an effect on spermatid transfer during male ejaculation. After insemination, male-derived spermatozoa, which are ~50% larger than those produced by hermaphrodites, crawl into the hermaphrodite spermatheca and have a competitive advantage over hermaphrodite-derived spermatozoa in fertilizing oocytes, so that self-fertilization is suppressed in wild-type animals (Ward and Carrel, 1979; LaMunyon and Ward, 1995; L'Hernault, 2006). *ced* mutant hermaphrodites, including *ced-1* and *ced-5* mutants, produced only cross-progeny when mated with wild-type males (supplementary material Fig. S5C). When *unc-76* hermaphrodites were mated with wild-type or *ced* mutant males at 36 hours post L4 stage, wild-type males gave rise to cross-progeny only but a mixture of Unc self-

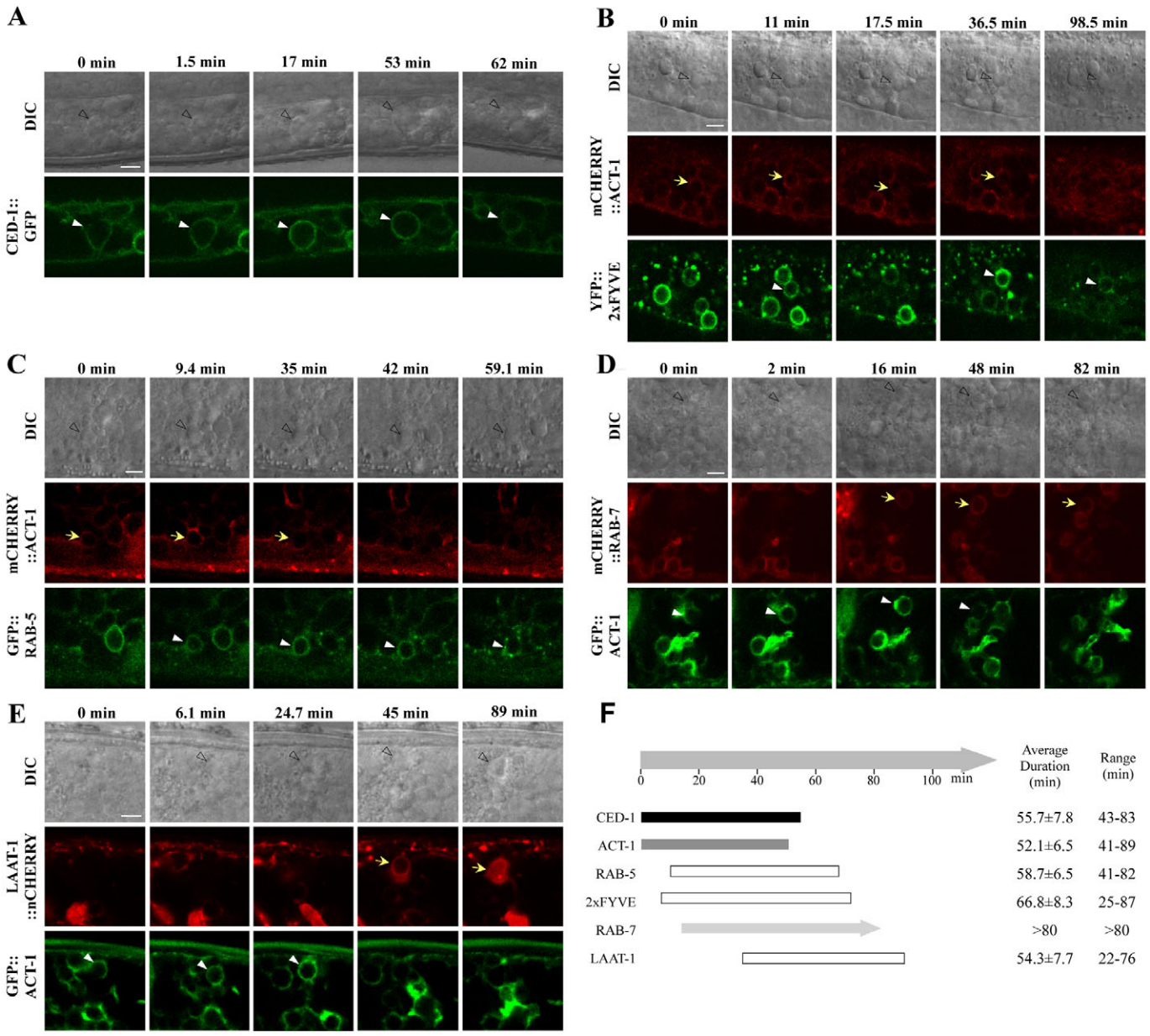

Fig. 4. Sequential recruitments of phagosome maturation factors to residual body-containing phagosomes. (**A-F**) DIC and confocal fluorescent images of wild-type animals expressing CED-1::GFP (A), mCHERRY::ACT-1 and YFP::2xFYVE (B), GFP::RAB-5 (C), GFP::ACT-1 and mCHERRY::RAB-7 (D) or LAAT-1::nCHERRY (E) at various time points. '0 min' indicates the time point when the mCHERRY::ACT-1 ring was just beginning to form (D,E) or had formed a complete ring (B,C). Quantification is shown in F. At least six phagosomes were examined for each reporter. Of the ten phagosomes examined, YFP::2xFYVE was recruited once, twice and multiple times to 5, 1 and 4 phagosomes, respectively. Yellow arrows, residual bodies labeled by red reporters; white arrowheads, residual bodies positive for green reporters; unfilled arrowheads, residual bodies observed by DIC. Scale bars: 5 μm.

progeny and non-Unc cross-progeny was generated from *ced* mutants (Fig. 6C). The defect of *ced-1* mutant males was rescued by the $P_{lim\text{-}7}$*ced-1::gfp* transgene (Fig. 6C). Males carrying both *lifeACT::RFP* and *his-72::GFP* transgenes showed that no residual bodies were passed from males into hermaphrodites during ejaculation (supplementary material Fig. S5A,B).

The generation of self- and cross-progeny by mutant males might be due to low sperm competitiveness or insemination of relatively few male-derived spermatids. An in vitro sperm activation assay by Pronase E indicated that ~92% of spermatids were activated in wild type or *ced* mutants (supplementary material Fig. S5D). *ced* mutant males showed normal male tail development, including extension of fans and generation of sensory rays and spicules that are essential for male mating (supplementary material Fig. S5E). To measure the number of spermatids in mating, mutant males were mated with *fog-2(q71); ceh-18(mg57)* females, in which the sperm-oocyte switch is defective and only oocytes are generated (Murray et al., 2011). The number of sperm transferred per ejaculation is thus determined by the number of progeny produced. Mating with wild-type males generated ~170 progeny, whereas *ced-1* and *piki-1* mutant males only gave rise to ~60 progeny. The $P_{lim\text{-}7}$*ced-*

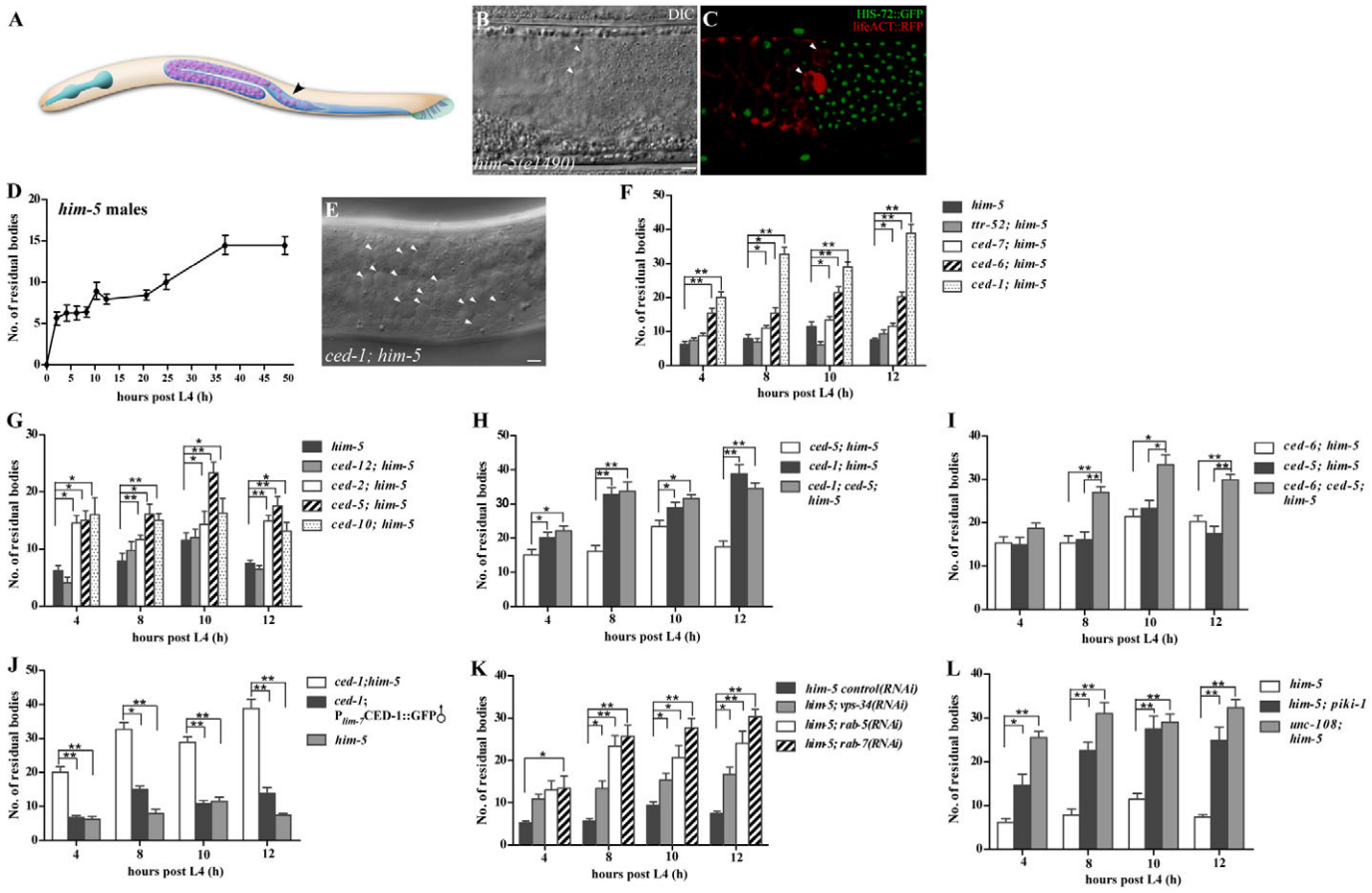

Fig. 5. Engulfment genes are differentially required for removing residual bodies in males. (**A**) Schematic of the male germline. Primary spermatocytes, residual bodies associated with non-budding spermatids and single spermatids are shown in the proximal gonad. (**B**,**C**) DIC (B) and fluorescence (C) images of a wild-type animal carrying P_{his-72}HIS-72::GFP and P_{pie-1}lifeACT::RFP. Residual bodies (arrowheads) are identified by their button-like morphology (B) and labeling by ACT-1::RFP but not HIS-72::GFP (C). (**D**) Residual bodies were scored in *him-5(e1490)* males at different time points (4, 8, 10, 12, 20, 24, 36 and 48 hours) post L4 stage. At least 15 worms were scored at each time point. (**E**) More residual bodies (arrowheads) accumulate in *ced-1(e1735)* mutant males. (**F-L**) Residual bodies were quantified in the indicated strains at different time points. At least 15 animals were scored for each strain at each time point. Data are shown as mean±s.e.m. $^{**}P<0.0001$; $^{*}P<0.05$. Scale bars: 5 μm.

1::gfp transgene partially rescued the defect of *ced-1* mutants, giving rise to ~155 progeny (Fig. 6D). These results indicate that excessive accumulation of residual bodies causes a defect in transfer of spermatids to hermaphrodites during mating.

DISCUSSION

Here, we revealed that the set of genes involved in apoptotic cell clearance in *C. elegans* also mediates the removal of residual bodies during spermatogenesis. Phagocytosis of residual bodies, which may be triggered by PS exposure on the surface, is mediated by two partially redundant engulfment pathways, and residual bodies are degraded through phagosome maturation, a process involving similar sequential recruitments of PtdIn(3)P and small GTPases as cell corpse degradation. Residual bodies in *Drosophila* and mammals display many features of apoptotic bodies (Arama et al., 2003; Blanco-Rodríguez and Martínez-García, 1999), including PS exposure on the surface of residual bodies that are recognized by class B scavenger receptor type I (Nakanishi and Shiratsuchi, 2004). In *Drosophila*, caspase activation and apoptosis-like events are required for efficient partition of cytoplasm into waste bags (residual bodies) during spermatid individualization (Arama et al., 2003). However, we found that loss of *ced-3*, *ced-4* or *egl-1*, the essential genes for cell death activation in worms, did not affect residual body removal, suggesting that the apoptotic program might not play a crucial role in this process.

Although a common set of genes is utilized for removal of embryonic cell corpses in hermaphrodites and males (supplementary material Fig. S5G), we found that the genes are differentially required for removing residual bodies (Fig. 6E). Residual bodies in hermaphrodites are removed by the same machinery in a very similar fashion to the clearance of apoptotic cells, albeit a little more slowly. In males, however, engulfment genes form a distinct hierarchy during residual body removal, with the CED-1 receptor acting upstream of both engulfment pathways. TTR-52, the secreted bridging molecule that cross-links the PS ‘eat me’ signal on apoptotic cells with the CED-1 receptor on phagocytes, and the ABC transporter CED-7, which is required for CED-1 clustering around cell corpses, appear to be dispensable for removing residual bodies in males, indicating that different regulatory components or mechanisms might be involved. The presence of multiple PS recognition mechanisms has been implicated by the milder defect of cell corpse removal in *ttr-52* mutants than in *ced-1* mutants (Wang et al., 2010). The removal of

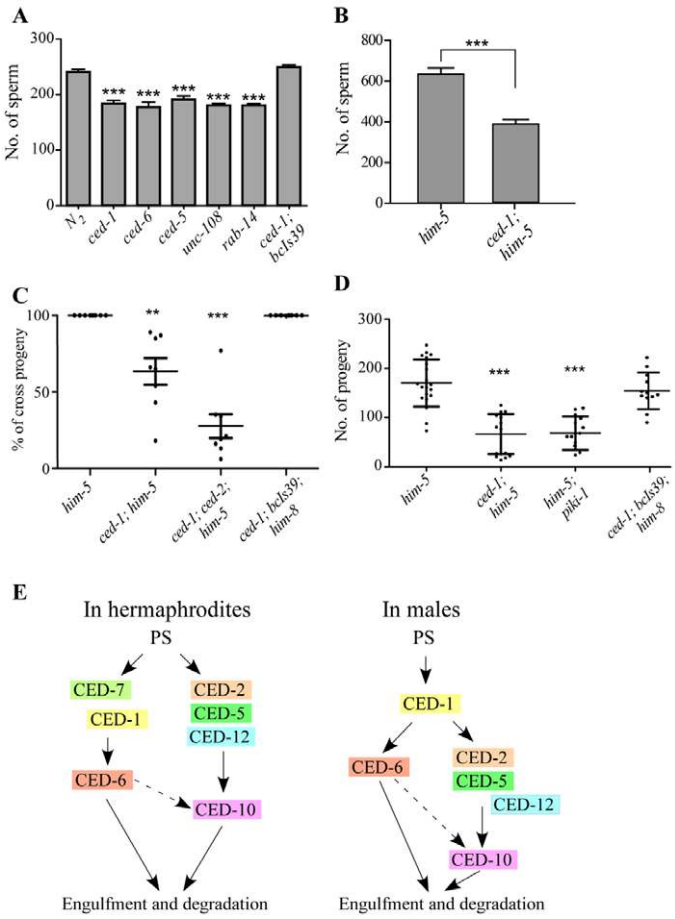

Fig. 6. Accumulation of residual bodies reduces the number of spermatids and impairs male mating efficiency. (**A**,**B**) The number of spermatids was quantified in hermaphrodites (4 hours post L4 stage, A) or males (10 hours post L4 stage, B) of the indicated strains. Animals in A and B carry the HIS-72::GFP transgene to facilitate spermatid counting. At least ten worms were scored for each strain. Data are shown as mean±s.d. ***P<0.001. (**C**) A mixture of Unc self-progeny and non-Unc cross-progeny are generated from *unc-76* hermaphrodites mated with mutant males 36 hours post L4 stage. Wild-type males give rise to only non-Unc cross-progeny. At least eight worms were tested for each strain. ***P<0.001; **P<0.01. The *ced-1; ced-2; him-5* triple mutants are less healthy compared with *ced-1; him-5* mutants. (**D**) Sperm transferred during mating was quantified in *fog-2; ceh-18* females mated with males of the indicated strains. At least ten worms were tested for each male strain. Data are shown as mean±s.e.m. ***P<0.001. (**E**) Summary of the two partially redundant engulfment pathways for residual body removal in hermaphrodites and males. In males, CED-7 is dispensable and CED-12 plays a minor role.

residual bodies is much more efficient in males than in hermaphrodites, which is consistent with the much higher level of spermatid generation in males (~3000 in males versus ~300 in hermaphrodites). In mammals, it has been proposed that residual body disposal is initiated by autophagy, with internalization and digestion carried out by Sertoli cells (Chemes, 1986). In *C. elegans*, however, autophagy seems not to play an essential role in residual body disposal.

We found that efficient removal of residual bodies is essential for sperm quantity and transfer. Mutants with defective removal of residual bodies contain reduced numbers of spermatids. During mating, engulfment mutant males transfer fewer spermatids into hermaphrodites. Although sperm from engulfment mutant males can be activated normally in vitro with Pronase E, they may be less competitive in vivo. Defective elimination of residual bodies in mammals is associated with impairment of sperm release and causes infertility (Sharpe et al., 1995; Zheng et al., 2007). Elimination of residual bodies may provide appropriate spaces for normal spermatogenesis and sperm transfer, whereas accumulation of residual bodies might suppress spermatogenesis. In addition, phagocytosis of residual bodies by gonadal sheath cells might promote spermatogenesis by providing a source of energy. Our study revealed the involvement of a common molecular mechanism in clearing apoptotic cells and removing residual bodies during *C. elegans* spermatogenesis.

Acknowledgements
We thank Drs Z. Bao, R. Waterson, C. Yang, K. S. Ravichandran and M. O. Hengartner, and the *Caenorhabditis* Genetic Center for strains; members of the Zhang and Wang laboratories for helpful comments on the manuscript; and Dr Isabel Hanson for editing services.

Funding
This work was supported by the National Basic Research Program of China [2011CB910100, 2010CB835201 to H.Z. and X.W.]. The research of X.W. and H.Z. was supported in part by International Early Career Scientist grants from the Howard Hughes Medical Institute. Deposited in PMC for release after 6 months.

Competing interests statement
The authors declare no competing financial interests.

Supplementary material
Supplementary material available online at
http://dev.biologists.org/lookup/suppl/doi:10.1242/dev.086769/-/DC1

References
Arama, E., Agapite, J. and Steller, H. (2003). Caspase activity and a specific cytochrome C are required for sperm differentiation in Drosophila. *Dev. Cell* **4**, 687-697.
Blanco-Rodríguez, J. and Martínez-García, C. (1999). Apoptosis is physiologically restricted to a specialized cytoplasmic compartment in rat spermatids. *Biol. Reprod.* **61**, 1541-1547.
Breucker, H., Schäfer, E. and Holstein, A. F. (1985). Morphogenesis and fate of the residual body in human spermiogenesis. *Cell Tissue Res.* **240**, 303-309.
Chemes, H. (1986). The phagocytic function of Sertoli cells: a morphological, biochemical, and endocrinological study of lysosomes and acid phosphatase localization in the rat testis. *Endocrinology* **119**, 1673-1681.
Gumienny, T. L., Lambie, E., Hartwieg, E., Horvitz, H. R. and Hengartner, M. O. (1999). Genetic control of programmed cell death in the Caenorhabditis elegans hermaphrodite germline. *Development* **126**, 1011-1022.
Gumienny, T. L., Brugnera, E., Tosello-Trampont, A. C., Kinchen, J. M., Haney, L. B., Nishiwaki, K., Walk, S. F., Nemergut, M. E., Macara, I. G., Francis, R. et al. (2001). CED-12/ELMO, a novel member of the CrkII/Dock180/Rac pathway, is required for phagocytosis and cell migration. *Cell* **107**, 27-41.
Guo, P., Hu, T., Zhang, J., Jiang, S. and Wang, X. (2010). Sequential action of Caenorhabditis elegans Rab GTPases regulates phagolysosome formation during apoptotic cell degradation. *Proc. Natl. Acad. Sci. USA* **107**, 18016-18021.
Hsu, T. Y. and Wu, Y. C. (2010). Engulfment of apoptotic cells in C. elegans is mediated by integrin alpha/SRC signaling. *Curr. Biol.* **20**, 477-486.
Kamath, R. S. and Ahringer, J. (2003). Genome-wide RNAi screening in Caenorhabditis elegans. *Methods* **30**, 313-321.
Kinchen, J. M. and Ravichandran, K. S. (2008). Phagosome maturation: going through the acid test. *Nat. Rev. Mol. Cell Biol.* **9**, 781-795.
Kinchen, J. M., Cabello, J., Klingele, D., Wong, K., Feichtinger, R., Schnabel, H., Schnabel, R. and Hengartner, M. O. (2005). Two pathways converge at CED-10 to mediate actin rearrangement and corpse removal in C. elegans. *Nature* **434**, 93-99.
L'Hernault, S. W. (2006). Spermatogenesis. In *WormBook* (ed. The C. elegans Research Community), www.wormbook.org.
LaMunyon, C. W. and Ward, S. (1995). Sperm precedence in a hermaphroditic nematode (Caenorhabditis elegans) is due to competitive superiority of male sperm. *Experientia* **51**, 817-823.
Liu, B., Du, H., Rutkowski, R., Gartner, A. and Wang, X. (2012). LAAT-1 is the lysosomal lysine/arginine transporter that maintains amino acid homeostasis. *Science* **337**, 351-354.

Liu, Q. A. and Hengartner, M. O. (1998). Candidate adaptor protein CED-6 promotes the engulfment of apoptotic cells in C. elegans. *Cell* **93**, 961-972.
Lu, Q., Zhang, Y., Hu, T., Guo, P., Li, W. and Wang, X. (2008). C. elegans Rab GTPase 2 is required for the degradation of apoptotic cells. *Development* **135**, 1069-1080.
Machaca, K., DeFelice, L. J. and L'Hernault, S. W. (1996). A novel chloride channel localizes to Caenorhabditis elegans spermatids and chloride channel blockers induce spermatid differentiation. *Dev. Biol.* **176**, 1-16.
Mangahas, P. M., Yu, X., Miller, K. G. and Zhou, Z. (2008). The small GTPase Rab2 functions in the removal of apoptotic cells in Caenorhabditis elegans. *J. Cell Biol.* **180**, 357-373.
Murray, R. L., Kozlowska, J. L. and Cutter, A. D. (2011). Heritable determinants of male fertilization success in the nematode Caenorhabditis elegans. *BMC Evol. Biol.* **11**, 99.
Nakanishi, Y. and Shiratsuchi, A. (2004). Phagocytic removal of apoptotic spermatogenic cells by Sertoli cells: mechanisms and consequences. *Biol. Pharm. Bull.* **27**, 13-16.
Parrish, J., Li, L., Klotz, K., Ledwich, D., Wang, X. and Xue, D. (2001). Mitochondrial endonuclease G is important for apoptosis in C. elegans. *Nature* **412**, 90-94.
Reddien, P. W. and Horvitz, H. R. (2000). CED-2/CrkII and CED-10/Rac control phagocytosis and cell migration in Caenorhabditis elegans. *Nat. Cell Biol.* **2**, 131-136.
Schedl, T. (1997). Developmental genetics of the germ line. In *C. elegans II* (ed. D. L. Riddle, T. Blumenthal, B. J. Meyer and J. R. Priess), pp. 241-269. Cold Spring Harbor, NY: Cold Spring Harbor Laboratory Press.
Sharpe, R. M., Maguire, S. M., Saunders, P. T., Millar, M. R., Russell, L. D., Ganten, D., Bachmann, S., Mullins, L. and Mullins, J. J. (1995). Infertility in a transgenic rat due to impairment of cytoplasmic elimination and sperm release from the Sertoli cells. *Biol. Reprod.* **53**, 214-226.
Sulston, J. E. and Horvitz, H. R. (1977). Post-embryonic cell lineages of the nematode, Caenorhabditis elegans. *Dev. Biol.* **56**, 110-156.
Sulston, J. E., Schierenberg, E., White, J. G. and Thomson, J. N. (1983). The embryonic cell lineage of the nematode Caenorhabditis elegans. *Dev. Biol.* **100**, 64-119.
Tian, Y., Li, Z. P., Hu, W. Q., Ren, H. Y., Tian, E., Zhao, Y., Lu, Q., Huang, X. X., Yang, P. G., Li, X. et al. (2010). C. elegans screen identifies autophagy genes specific to multicellular organisms. *Cell* **141**, 1042-1055.
Wang, X., Wu, Y. C., Fadok, V. A., Lee, M. C., Gengyo-Ando, K., Cheng, L. C., Ledwich, D., Hsu, P. K., Chen, J. Y., Chou, B. K. et al. (2003). Cell corpse engulfment mediated by C. elegans phosphatidylserine receptor through CED-5 and CED-12. *Science* **302**, 1563-1566.
Wang, X., Wang, J., Gengyo-Ando, K., Gu, L., Sun, C. L., Yang, C., Shi, Y., Kobayashi, T., Shi, Y., Mitani, S. et al. (2007). C. elegans mitochondrial factor WAH-1 promotes phosphatidylserine externalization in apoptotic cells through phospholipid scramblase SCRM-1. *Nat. Cell Biol.* **9**, 541-549.
Wang, X., Li, W., Zhao, D., Liu, B., Shi, Y., Chen, B., Yang, H., Guo, P., Geng, X., Shang, Z. et al. (2010). Caenorhabditis elegans transthyretin-like protein TTR-52 mediates recognition of apoptotic cells by the CED-1 phagocyte receptor. *Nat. Cell Biol.* **12**, 655-664.
Ward, S. (1986). Asymmetric localization of gene products during the development of C. elegans spermatozoa. In *Gametogenesis and the Early Embryo 44th Symposium of the Society for Developmental Biology* (ed. J. G. Gall), pp. 55-75. New York, NY: Alan R. Liss.
Ward, S. and Carrel, J. S. (1979). Fertilization and sperm competition in the nematode Caenorhabditis elegans. *Dev. Biol.* **73**, 304-321.
Ward, S., Hogan, E. and Nelson, G. A. (1983). The initiation of spermiogenesis in the nematode Caenorhabditis elegans. *Dev. Biol.* **98**, 70-79.
Wu, Y. C. and Horvitz, H. R. (1998a). The C. elegans cell corpse engulfment gene ced-7 encodes a protein similar to ABC transporters. *Cell* **93**, 951-960.
Wu, Y. C. and Horvitz, H. R. (1998b). C. elegans phagocytosis and cell-migration protein CED-5 is similar to human DOCK180. *Nature* **392**, 501-504.
Wu, Y. C., Tsai, M. C., Cheng, L. C., Chou, C. J. and Weng, N. Y. (2001). C. elegans CED-12 acts in the conserved crkII/DOCK180/Rac pathway to control cell migration and cell corpse engulfment. *Dev. Cell* **1**, 491-502.
Yu, X., Odera, S., Chuang, C. H., Lu, N. and Zhou, Z. (2006). C. elegans Dynamin mediates the signaling of phagocytic receptor CED-1 for the engulfment and degradation of apoptotic cells. *Dev. Cell* **10**, 743-757.
Zhang, Y., Wang, H., Kage-Nakadai, E., Mitani, S. and Wang, X. (2012). C. elegans secreted lipid-binding protein NRF-5 mediates PS appearance on phagocytes for cell corpse engulfment. *Curr. Biol.* **22**, 1276-1284.
Zheng, H., Stratton, C. J., Morozumi, K., Jin, J., Yanagimachi, R. and Yan, W. (2007). Lack of Spem1 causes aberrant cytoplasm removal, sperm deformation, and male infertility. *Proc. Natl. Acad. Sci. USA* **104**, 6852-6857.
Zhou, Z. and Yu, X. (2008). Phagosome maturation during the removal of apoptotic cells: receptors lead the way. *Trends Cell Biol.* **18**, 474-485.
Zhou, Z., Caron, E., Hartwieg, E., Hall, A. and Horvitz, H. R. (2001a). The C. elegans PH domain protein CED-12 regulates cytoskeletal reorganization via a Rho/Rac GTPase signaling pathway. *Dev. Cell* **1**, 477-489.
Zhou, Z., Hartwieg, E. and Horvitz, H. R. (2001b). CED-1 is a transmembrane receptor that mediates cell corpse engulfment in C. elegans. *Cell* **104**, 43-56.
Zou, W., Lu, Q., Zhao, D., Li, W., Mapes, J., Xie, Y. and Wang, X. (2009). Caenorhabditis elegans myotubularin MTM-1 negatively regulates the engulfment of apoptotic cells. *PLoS Genet.* **5**, e1000679.